Spontaneous mode locking of a multimode semiconductor laser under continuous wave operation

Baptiste Chomet, Stéphane Blin, Grégoire Beaudoin, Konstantinos Pantzas, Isabelle Sagnes, Stéphane Denet, Arnaud Garnache

frontiers | Frontiers in Photonics

TYPE Brief Research Report
PUBLISHED 21 March 2023
DOI 10.3389/fphot.2023.1160251

OPEN ACCESS

EDITED BY
Anbang Wang,
Taiyuan University of Technology, China

REVIEWED BY
Pablo Marin-Palomo,
Vrije University Brussels, Belgium
Song-Sui Li,
Southwest Jiaotong University, China

*CORRESPONDENCE
Arnaud Garnache,
arnaud.garnache-creuillot@umontpellier.fr

SPECIALTY SECTION
This article was submitted to Non-linear Optics, a section of the journal Frontiers in Photonics

RECEIVED 06 February 2023
ACCEPTED 06 March 2023
PUBLISHED 21 March 2023

CITATION
Chomet B, Blin S, Beaudoin G, Pantzas K, Sagnes I, Denet S and Garnache A (2023), Spontaneous mode locking of a multimode semiconductor laser under continuous wave operation. *Front. Photonics* 4:1160251. doi: 10.3389/fphot.2023.1160251

Spontaneous mode locking of a multimode semiconductor laser under continuous wave operation

Baptiste Chomet[1,2], Stéphane Blin[1], Grégoire Beaudoin[3], Konstantinos Pantzas[3], Isabelle Sagnes[3], Stéphane Denet[2] and Arnaud Garnache[1]*

[1]CNRS UMR 5214, Institut d'Electronique et des Systèmes (IES), Université de Montpellier, Montpellier, France, [2]Innoptics, Institut d'Optique d'Aquitaine, Talence, France, [3]C2N, CNRS UMR9001, Université Paris-Saclay, Palaiseau, France

Self-starting mode-locking is observed in a laser based on a compact III-V diode-pumped quantum-well surface-emitting semiconductor laser technology with a saturable-absorber-free but dispersive cavity. Continuous wave generation of picosecond pulses at a rate of 100 GHz is demonstrated by recording microwave intensity noises, beat frequency, time-resolved optical spectra, and intensity autocorrelation. Coherence of the pulse train is obtained through the frequency noise measurement of the demodulated beat note, demonstrating a timing jitter as low as 110 fs, near the quantum limit. Using a theoretical model based on a generalized Haus master equation, we demonstrate the existence of this mode locked state without the need for saturable absorption. The fundamental physical mechanism is the interplay between self-phase modulation and anomalous dispersion like in cavity soliton together with light–matter interaction-induced time symmetry breaking.

KEYWORDS

semiconductor laser, VECSEL, dynamics, frequency combs, dispersion, non-linear

1 Introduction

Semiconductor mode-locked diode lasers (MLLDs) generating short pulses show potential in many applications, such as high-speed optical interconnects (Keeler et al., 2003; Keeler et al., 2003) or optical time domain multiplexing (Jiang et al., 2007; Mollenauer et al., 2000). In contrast with active MLLDs (Bowers et al., 1989), passive MLLDs do not require any external electrical oscillator. Passive mode-locking has been achieved in semiconductor lasers by the use of strongly intensity-dependent elements in the laser cavity where saturable absorption provides a coupling mechanism between laser modes, which typically results in short pulses in the time domain with repetition rates ranging from a few to hundreds of GHz (Marsh & Portnoi, 2000; Vladimirov & Turaev, 2004). However, owing to the spontaneous emission noise and their low-finesse cavity, MLLDs' optical pulse train exhibit significant phase noise and timing jitter (Hou et al., 2011). In contrast to edge-emitting devices, passively mode-locked vertical-external-cavity surface-emitting lasers (VECSELs) are sources of sub-ps pulse trains with excellent low jitter in a high beam quality (Garnache et al., 2002). In particular, the so-called mode-locked integrated external-cavity surface-emitting laser (MIXSEL), in which both the gain and the saturable absorber share the same microcavity, represents a compact source with a repetition rate up to 100 GHz (Maas et al., 2007). However, the gain and absorber layers, which require different

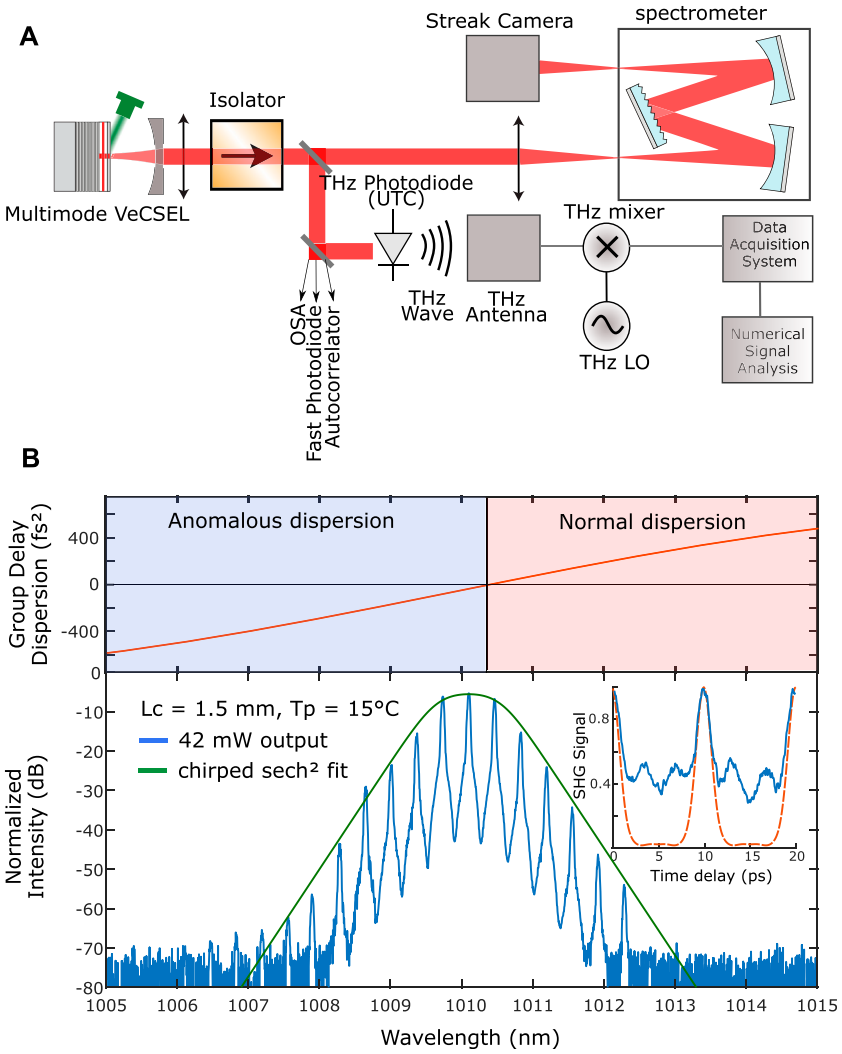

FIGURE 1
(A) Experimental setup for the characterization of the multimode VECSEL dynamics. **(B)** Top plot, calculated second-order dispersion of the microcavity VECSEL. Bottom plot, optical spectrum of the laser for an optical output power of 42 mW and the fit of the state with a spectral sech2 envelope. Inset: Intensity autocorrelation signal obtained through second harmonic generation (blue) and calculated from the sech2 envelope (red).

quantum confinements, have to be optimized separately by using different growth parameters.

On the other hand, mode-locking can also occur in semiconductor lasers in the absence of a saturable absorber (Day et al., 2020; Sato, 2003; Rosales et al., 2012). In this case, it is understood that the beating of different laser modes leads to oscillations of the carrier density in the gain medium at multiples of the repetition frequency (corresponding to longitudinal mode spacing), which, in turn, again couple with the laser modes. In the presence of spatial inhomogeneous gain saturation (spatial hole burning), this locking phenomenon leads to frequency modulation rather than amplitude modulation, even though self-generation of optical pulses has been reported in single-section quantum-dash lasers (Gosset et al., 2006).

In this article, we report a self-starting mode-locked system generating picosecond pulses at a rate of 100 GHz based on an absorber free short cavity VECSEL. Stable mode-locked operation is triggered by an instability known in the framework of the complex Ginzburg–Landau equation (CGLE) as phase turbulence (Gil & Lippi, 2014). It predicts that a semiconductor laser can undergo a transition to a multimode regime due to non-linearity and phase dispersion. In the absence of spatial hole burning (SHB), this coherent non-linear process gives rise to phase-locked frequency combs first observed in quantum cascade lasers (Piccardo et al., 2020). In a VECSEL, as the quantum well (QW) thickness is very small compared to the wavelength and QWs are usually located at the antinodes of the laser electric field, all the modes are in phase on the gain medium. This prevents longitudinal SHB, and thanks to the QWs homogeneous broadened gain, the multi-longitudinal dynamics is only driven by coherent non-linear mode–mode coupling (Garnache et al., 2007; Chomet et al., 2023). Here, we take advantage of the VECSEL technology and physical concept advantages to precisely engineer the amount of phase dispersion in

the laser cavity. The signature of a stable comb regime is demonstrated through time resolved optical spectra and a narrow beating at the mode spacing frequency by excitation of a uni-traveling-carrier photodiode. The latter is shown to have a phase noise near the quantum limit. Using a generalized Haus master equation (HME), we reproduce this stable locked state and discuss the impact of gain recovery on dynamics.

2 Methods

The laser cavity shown in Figure 1A includes a GaA-based gain mirror and an output coupler (99%) separated by an air gap of L_c = 1.5 mm , leading to a free spectral range (FSR) of 100 GHz. The gain structure (GaAs 229) is temperature-stabilized thanks to a Peltier cooler and optically pumped by a 808-nm 400-mW low-noise single-mode diode on a radius of 30 μm (at $\sim 70°$ Brewster angle). A 1.1λ/4 SiN thick antireflection coating is deposited on the top surface to reduce the microcavity resonance filtering effect on gain bandwidth and to introduce the anomalous group velocity dispersion essential for triggering comb formation. The calculated spectral dependence of the dispersion is shown in Figure 1B. More details about the gain structure and dispersion calculation can be found in Supplementary Material S1.

The laser operates at a Peltier temperature $T_p = 15^{\circ}C$ in continuous wave (cw) at a wavelength of $\sim$ 1.01 μm. Laser emission is reached for a threshold density of 1.8 kW/cm^2, and a maximum output power of 60 mW is achieved. The laser beam is collimated using a 75-mm-focal achromatic lens, followed by the application of an optical isolator to prevent parasitic feedback. Just above the laser threshold, the device emits in a single longitudinal mode. However, for an output power of 42 mW, the spectrum (Figure 1B) consists of a few strong modes superimposed on a sech^2-shaped lobe. The peak of the spectrum arises close to the zero-crossing of the dispersion in the anomalous dispersion regime. The generation of a pulse train was indicated by using a background free auto-correlator (FR-103XL) with a delay of 150 ps (inset of Figure 1B). Pulse to pulse duration was 10 ps, which corresponds to a round-trip time of the cavity. The second harmonic generated (SHG) signal reached 60% of modulation, meaning that continuum is still present. The dotted line is the SHG profile calculated from the Fourier transform of the optical spectrum, which is close to the measured one at the vicinity of the peak maxima, demonstrating the stabilization close to the Fourier transform limited pulses. The calculated pulse width was 1.4 ps (FWHM).

Although the SHG signal strongly indicates the presence of a pulse train, stability of the comb lines has to be evaluated to confirm stable mode locking. Here, we employed two techniques, time-resolved spectra and RF spectra of the pulse train. The experimental setup is shown in Figure 1A.

3 Results

3.1 Observation of a highly coherent self-mode-locked light state

The first confirmation of mode locking was obtained by recording the cw optical spectrum at the output of a high-resolution grating monochromator (JY HR1000), using a streak camera (Hamamatsu C10910-02) with a time resolution of 25 ns, as shown in Figure 2A. The single-shot trace shows a cw operation for the comb lines, with a frequency difference of approximately 100 GHz (resolution of 25 GHz). Detuning the peak of the spectrum with respect to the zero-crossing of the dispersion leads to an unstable behavior of the comb where fast-intensity oscillations of each mode are observable (Figure 2B). Signature of these oscillations at ~4.5 MHz (and higher harmonics) was visible in the total laser output intensity fluctuations recorded with a 2-GHz bandwidth low-noise photodiode for 1.2 mA of photocurrent (Figure 2C). In the mode-locked regime, intensity noise is pump noise limited up to the laser cut-off frequency (~120 MHz) and reaches above the shot noise level. The pulse train is then very stable with relative *rms* intensity fluctuations below 0.1% in the 100 kHz–1 GHz frequency range.

Second confirmation of mode locking was obtained by recording the RF spectra of the pulse train by excitation of a commercial uni-traveling-carrier photodiode (IOD-PMAN-13001-1 from NTT) (Blin et al., 2017). The microwave signal that comes from the photodiode is collimated using a 10-cm focal-length Teflon lens, then focused using an identical lens into a calibrated heterodyne head receiver that allows observation of the beating at the round-trip frequency on a RF analyzer, as shown in the inset of Figure 2D. The center frequency was 111.24 GHz, and the linewidth was $<$ 200 kHz for a 10-ms measuring time, which tends to be limited by the 100-kHz resolution bandwidth of the RF analyzer. This beat note was then downshifted below 1 GHz and amplified using a 20-dB-gain 0.1–1 GHz bandwidth low-noise amplifier (Minicircuit ZFL-1000LN). More details about the setup can be found in Supplementary Material and Supplementary Section S2. The resulting signal was then analyzed thanks to a numerical Hilbert transform, in order to extract the single-sided spectral density of phase-noise fluctuations, as described by Bandel et al. (2016). The result is shown in Figure 2D together with its quantum limited case calculated from Paschotta et al. (2006). From this, we obtained an integrated timing jitter δT of 110 fs in a bandwidth of 1 kHz–1 MHz (Haus & Mecozzi, 1993; Scott et al., 2001). This low value has to be related to the high repetition rate of the pulse and gives an absolute jitter $\delta T/T \sim 1\%$, which is higher by two orders of magnitude than typical values obtained by SESAM mode-locked VECSELs with the GHz repetition rate in approximately the same integration bandwidth ($\delta T/T \sim 0.01\%$) (Wittwer et al., 2011; Quarterman et al., 2008). Nevertheless, in our case, the phase relationships between the modes are ultra-stable as the phase noise reaches its quantum limit above 10 kHz of RF frequency (see Figure 2D). The laser then emits a highly coherent train of picosecond pulses, the timing jitter of which is close to its quantum limited case (90 fs). This demonstrates that the non-linear process that triggers this locked state is highly coherent. However, we experimentally found that a stable comb formation occurs only for a short range of dispersion, as discussed previously (Figures 2B, C).

3.2 Justification of the existence of self-starting frequency combs

To confirm that the observed locked state is a result of the interplay between anomalous dispersion and non-linear phase

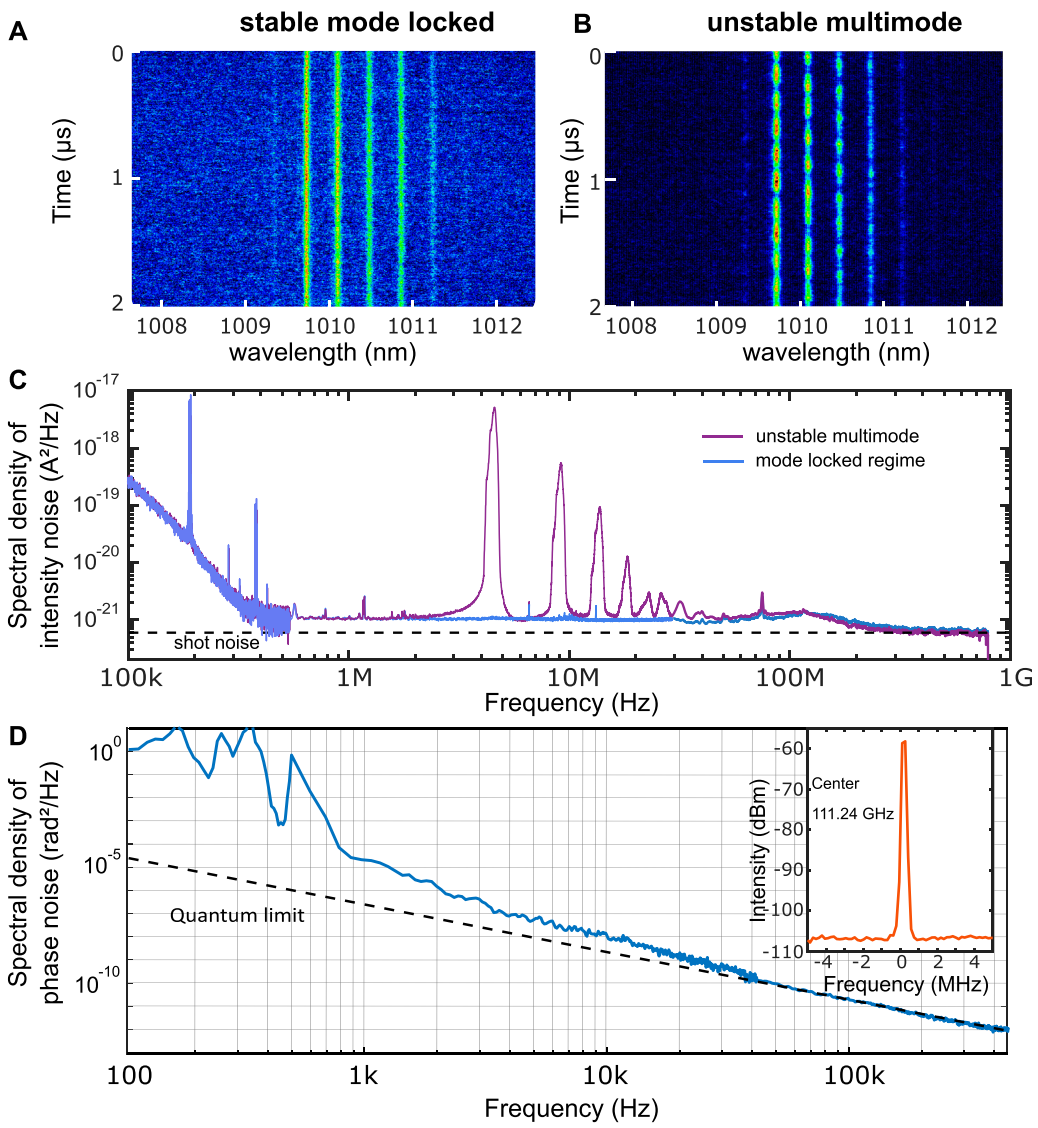

FIGURE 2
Optical spectrum time dependence (single-shot) observed with a temporal resolution of 25 ns and a spectral resolution of 25 GHz in the mode-locked state **(A)** and unstable state **(B)**. **(C)** RF spectrum of the laser output intensity fluctuations in the mode-locked and unstable regime. In the latter, oscillations of the modal intensity occur at ~4.5 MHz and harmonics. **(D)** Optical phase noise power spectral density of the demodulated beat note. The quantum-limited case is also plotted in the dashed line. Inset: RF spectrum of the 111.24 -GHz beat note for a 100-kHz resolution bandwidth and a 10-ms sweep time of the spectrum analyzer.

changes, we simulate the laser dynamics using a generalized HME (Hausen et al., 2020). Such an equation can be reduced to the CGLE that has been shown to support comb formation in the case where ultrafast gain relaxation and near-threshold operation are considered. The latter considerations are not suitable with our device as comb formation occurs well above the laser threshold and the carrier lifetime is much longer than the cavity round–trip time. The generalized HME reads as follows:

$$\partial_\xi A = \frac{1}{2}\left[(1-i\alpha)G - G_0\right]A + \frac{1}{2}\frac{4G_0}{\gamma^2 T^2}\partial_t^2 A + i\Sigma_1^n \frac{i^n}{T^n n!}\Phi_n \partial_t^n A, \quad (1)$$

$$\partial_t G = \gamma_e T\left(G_0\eta - G - G|A|^2\right), \quad (2)$$

$$\partial_\xi G = \gamma_e T G_0 \eta - \gamma_e T \int_0^1 G\left(1+|A|^2\right)dt, \quad (3)$$

with ξ being an integer describing the evolution from one round-trip toward the next; it represents a slow time scale, while the second variable t refers to the time evolution normalized to one round-trip. Eq. 1 (Keeler et al., 2003) describes the electric field evolution from round-trip to round-trip $\partial_\xi A$ and the variation of the carrier G on the fast time scale t. Eq. 3 is used to maintain the long-term carrier dynamics. Here, γ_e is the carrier relaxation rate in the gain, γ is the gain bandwidth, G_0 is the unsaturated gain (Loss), α is the amplitude phase coupling, η is the pump over the threshold ratio, and T is the cold cavity round-trip time. Φ_n are the different orders of phase dispersion. Here, we consider the expansion until $n = 3$. Phase dispersion in VECSEL cavities is mainly introduced through the amplitude reflectivity of the gain mirror, which acts as a Gires–Tournois interferometer (GTI). Thus, phase dispersion can

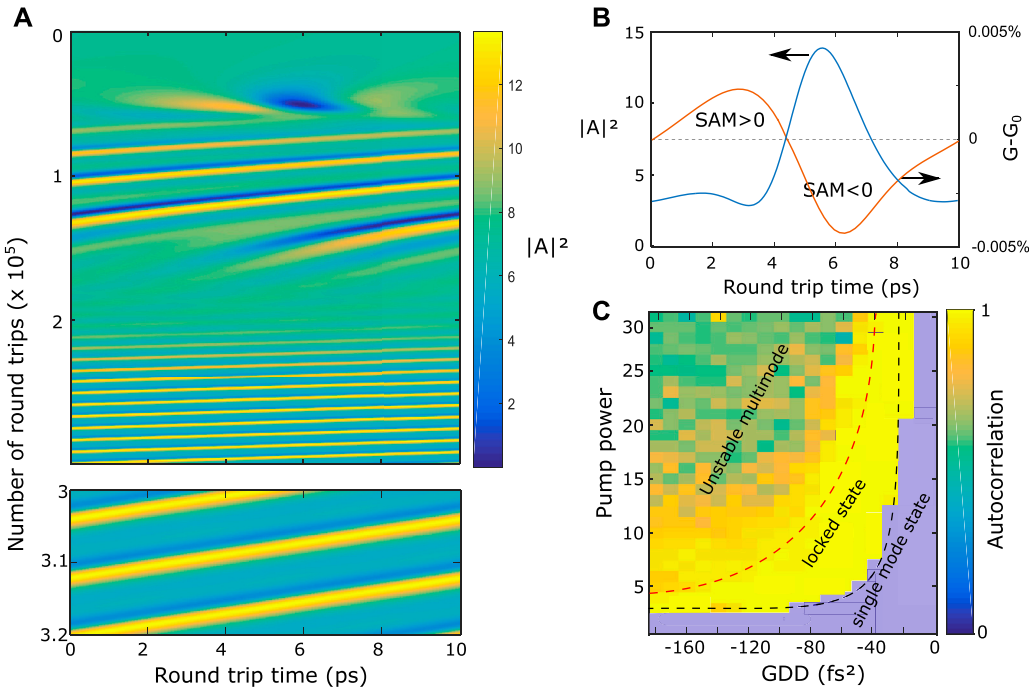

FIGURE 3
(A) Space–time simulation of the laser dynamics, showing the intensity in the cavity at every round-trip. Simulation parameters are (γ_e, γ, T, G_0, α, η, Φ_1, Φ_2, Φ_3) = ($1\times10^9 s^{-1}$, $2.8\times10^{13} s^{-1}$, 10 ps, 0.01, 2, 8, 80 fs, −80 fs^2, and −53000 fs^3). **(B)** Profile of the field intensity $|A|^2$ and gain G fluctuations at a steady state. **(C)** Calculated autocorrelation as both the pump ratio η and second-order dispersion (GDD) are tuned. Comb formation is obtained in the region between the black and red dashed lines.

be precisely engineered through the round-trip time of the microcavity and top VECSEL reflection coefficient (see Supplementary Material S1). For example, the impact of third-order dispersion (TOD) has been demonstrated in the multi-longitudinal dynamics of a MIXSEL (Schelte et al., 2020). Evaluating the phase reflectivity of our gain structure at the vicinity of the lasing wavelength, we consider a time delay Φ_1 = 80 fs, group velocity dispersion (GDD) Φ_2 = −80 fs^2, and a TOD Φ_3 = −53000 fs^3.

The resulting Eqs 1–3 were solved using standard split-step methods, such as the outlined method, for example, by Gurevich and Javaloyes (2017). Figure 3A shows the two time scale representations of the dynamics of the laser output intensity. After a relatively long time interval (about 200,000 round-trips) the laser reaches a frequency comb regime, where a single pulse is stabilized in the cavity. Strong gain depletion and time symmetry breaking terms (time delay and TOD) induce a drift of the pulse within the cavity (Javaloyes et al., 2016). The lack of time symmetry can also be seen in Figure 3B, where the pulse shows an asymmetric profile because of the long time response of the medium. The pulse FWHM is ~2 ps and lies on a continuum background in good agreement with autocorrelation measurements (Figure 1B). Experiments indicate that a precise control of the GDD is needed to generate this highly coherent state, and we investigate its stability in the parameter space GDD-η. Figure 3C displays a colormap of the calculated autocorrelation of the laser intensity. The autocorrelation in this context means that we compare the intensity over one round-trip with the intensity delayed by several round trips. In a comb, they match perfectly, and the autocorrelation is exactly unity. A part of the parameter space is a single frequency state (gray area), and instability of this solution (black dash line) occurs for an amount of anomalous dispersion given by $GDD < -\frac{1}{\alpha}4G_0/\gamma^2 \sim -25$ fs^2 (Chomet et al., 2023). This instability generates intensity fluctuations that grow with an increase of GDD in a strictly periodic manner, generating a comb. In the absence of fast positive self-amplitude modulation (SAM), thanks to a saturable absorber process, this stable pulsed state finds its origin in time symmetry breaking under weak gain—SAM—saturation/modulation. Thus, a short pulse is allowed to propagate with causality principle breaking by drifting strongly backward to maximize the amplification gain ($>$ 0 SAM), as seen in Figures 3A, B. This pulse regime will thus be slightly red shifted. We believe that in this light state, GDD dispersion tends to balance self-phase modulation (SPM) associated with the amplitude phase coupling factor as in the soliton-like laser mode-locking mechanism (Zolotovskii et al., 2015). The typical value of pulse duration $\delta\tau$ in this mode-locked regime at the vicinity of the next unstable region is as follows:

$$\delta\tau = 2\pi\sqrt{\frac{2|GDD|}{\alpha\gamma_e TG_0(\eta-1)}}. \tag{4}$$

Equation 4 is analogous to that describing the width of a fundamental soliton, where $\alpha\gamma_e TG_0$ is the effective SPM coefficient. With the values of Figure 3B, $\delta\tau$ ~2.1 ps is in good agreement with the width of the pulse shown. Equation 4 dictates an

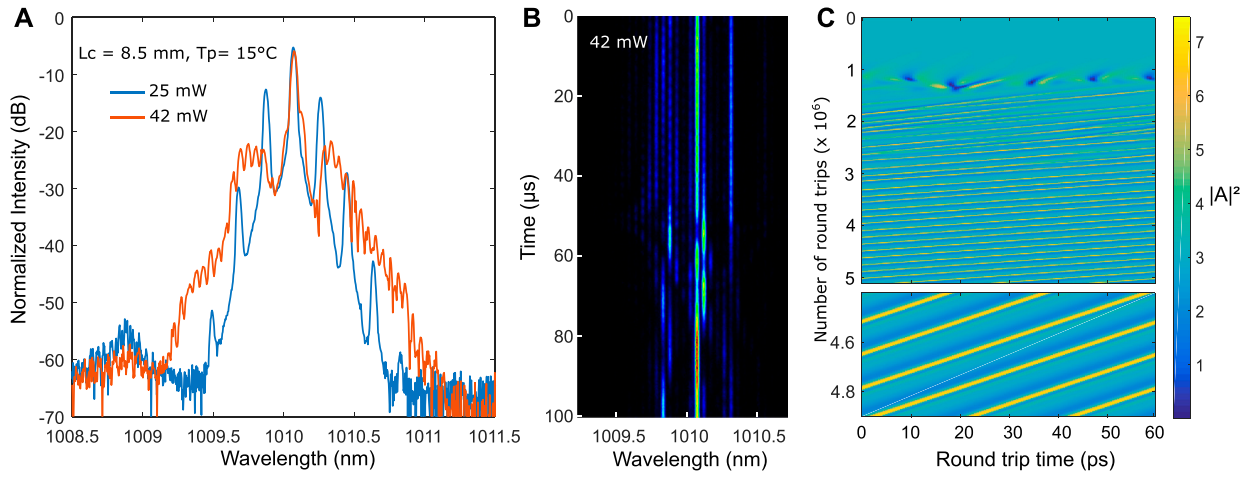

FIGURE 4
(A) Laser optical spectrum in the long cavity configuration (L_c = 8.5 mm) for output power 42 mW (red) and 27 mW (blue). **(B)** Optical spectrum time dependence (single-shot) observed with a temporal resolution of 250 ns and a spectral resolution of 14 GHz for 42 mW). **(C)** Space–time simulation of the laser intensity. Simulation parameters are similar to those of Figure 3A but T = 60 ps, η = 4, and Φ_2 = −60 fs². In this long cavity configuration, the laser stabilizes three pulses within a round-trip, resulting in a regime of harmonic mode locking.

ever-decreasing pulse width for increasing pumping power or cavity round-trip time. This only works until the pulse experiences very strong losses due to the finite-gain bandwidth. The pulse will then break in a double-pulse solution such that each pulse is longer and experiences a reduced loss due to the filter. To show this, we investigate the mode-locking behavior of the laser with an increase in the cavity length. Increasing the latter will result in the gain responding faster to the electric field beating at the cavity round-trip frequency, and thus, a larger SPM coefficient.

Figure 4A shows the optical spectrum of the laser operating in the anomalous dispersion regime close to zero GDD (in blue P_{out} = 27 mW, in red P_{out} = 42 mW) in a long cavity configuration L_c = 8.5 mm (FSR = 18 GHz). The spectrum corresponding to P_{out} = 27 mW (blue curve in Figure 4A) shows a mode spacing ~54 GHz = 3 × FSR, which suggests a regime of harmonic mode locking (HML), where three pulses instead of one circulate in the cavity. Increasing the pump power leads to oscillation of more cavity modes (red curve in Figure 4A), but a streak camera photograph reveals an unstable behavior of the optical spectrum (Figure 4B). Figure 4C presents the results of numerical simulations of Eqs 1–3 (Keeler et al., 2003; Keeler et al., 2003; Jiang et al., 2007), which confirms the experimental observations in which the laser intensity is now seen to stabilize not a single but three pulses within the cavity. This stable HML regime is, however, easily destabilized with a change of the control parameters (pumping power, dispersion, cavity length…), which results in pulses drifting with different group velocities. We show in Supplementary Section S3 that a non-null third-order dispersion is necessary to stabilize this multiple pulse solution; this is interesting as TOD is, here again, a parameter that can be engineered.

4 Discussion

In summary, we have presented a regime of spontaneous mode locking in a short cavity VECSEL. A train of pulses with a low timing jitter was demonstrated to be generated in the cavity. Existence of this comb regime was demonstrated by a generalized HME. Its formation is due to the interplay with dispersion and a slow light–matter interaction that induces time symmetry breaking and positive SAM even in the absence of a saturable absorber. Increasing the cavity length was seen to result in a breakup into multiple pulses and a regime of HML. Stabilization of the latter could possibly be engineered with TOD. In contrast with MIXSEL, where the gain and absorber layers have to be carefully optimized, here, we have used a common GaA-based gain mirror, where phase dispersion can be tailored by dielectric coatings. The use of metamaterials could also lead to a fine tuning of the dispersive effects.

We believe this spontaneous mode-locking laser regime could be observed in other slow gain laser materials with $\gamma_e T\,(\eta - 1) < 1$ at a repetition rate $1/T$ in the presence of phase amplitude coupling: a ns pulse train at 110 MHz has been observed in a cw traveling wave Ti: sapphire laser system including a spectral filter but was attributed to the Kerr lens effect, whereas below the Kerr non-linearity intensity threshold (Akachanov & Fstoeckel, 1995), an unstable mode locking at 100 MHz has been observed in a ring dye laser under strong dispersion (Vinogradov et al., 1992). A frequency comb at 11 GHz has been demonstrated based on a dispersive QCL ring micro-resonator (Piccardo et al., 2020), but in this Kerr-like fast media system $\gamma_e T > 1$, an HML regime takes place.

An interesting application of such spontaneous mode-locking processes characterized by a low non-linear intensity threshold < 10 kW/cm² would be to seed the start of the passively mode-locked system exhibiting a high non-linear SAM threshold intensity above ≫ 10 kW/cm² (like in Kerr-based mode locking).

Data availability statement

The raw data supporting the conclusion of this article will be made available by the authors, without undue reservation.

Author contributions

BC conducted the experiments and contributed to the writing of the manuscript and the interpretation of results. SB contributed to the experiments and to the interpretation of the results. GB, KP, and IS fabricated the semiconductor structure. SD supervised the work. AG supervised the work and contributed to the writing of the manuscript and the interpretation of results. All authors contributed to the article and approved the submitted version.

Funding

The authors acknowledge the French RENATECH network and the Agence Nationale de la Recherche (ANR-18-CE24-BLASON, ANR-19-CE24-SPATIOTERA, and ANR-16-ASTR-TAPAS), ANRT and I-SITE MUSE AAP2021 (STAE).

Acknowledgments

The authors thank Mikhaël Myara (IES) for his help in noise measurements, J. Javaloyes (UIB) and A. Vladimirov (WIAS) for fruitful discussions on the theoretical model.

Conflict of interest

Authors BC and SD were employed by Innoptics.

The remaining authors declare that the research was conducted in the absence of any commercial or financial relationships that could be construed as a potential conflict of interest.

Publisher's note

All claims expressed in this article are solely those of the authors and do not necessarily represent those of their affiliated organizations, or those of the publisher, the editors, and the reviewers. Any product that may be evaluated in this article, or claim that may be made by its manufacturer, is not guaranteed or endorsed by the publisher.

Supplementary material

The Supplementary Material for this article can be found online at: https://www.frontiersin.org/articles/10.3389/fphot.2023.1160251/full#supplementary-material

References

Akachanov, A., and Fstoeckel (1995). Intracavity laser spectroscopy with vibronic solid state lasers: Ii. influence of the nonlinear mode coupling on the maximum sensitivity of a ti: sapphire laser. *J. Opt.Soc.Am.B* 12, 970–979. doi:10.1364/josab.12.000970

Bandel, N. V., Myara, M., Sellahi, M., Souici, T., Dardaillon, R., and Signoret, P. (2016). Time-dependent laser linewidth: Beat-note digital acquisition and numerical analysis. *Opt. Express* 24, 27961–27978. doi:10.1364/OE.24.027961

Blin, S., Paquet, R., Myara, M., Chomet, B., Le Gratiet, L., Sellahi, M., et al. (2017). Coherent and tunable thz emission driven by an integrated iii–v semiconductor laser. *IEEE J. Sel. Top. Quantum Electron.* 23, 1–11. doi:10.1109/jstqe.2017.2654060

Bowers, J., Morton, P., Mar, A., and Corzine, S. (1989). Actively mode-locked semiconductor lasers. *IEEE J. Quantum Electron.* 25, 1426–1439. doi:10.1109/3.29278

Chomet, B., Vigne, N., Beaudoin, B., Pantzas, K., Blin, S., Sagnes, I., et al. (2023). Nonlinear dynamics of multimode semiconductor lasers: Dispersion based phase instability and route to single frequency operation. *Opt. Lett.* doi:10.1364/OL.482138

Day, M. W., Dong, M., Smith, B. C., Owen, R. C., Kerber, G. C., Ma, T., et al. (2020). Simple single-section diode frequency combs. *Apl. Photonics* 5, 121303. doi:10.1063/5.0033211

Garnache, A., Hoogland, S., Tropper, A. C., Sagnes, I., Saint-Girons, G., and Roberts, J. S. (2002). Sub-500-fs soliton-like pulse in a passively mode-locked broadband surface-emitting laser with 100 mw average power. *Appl. Phys. Lett.* 80, 3892–3894. doi:10.1063/1.1482143

Garnache, A., Ouvrard, A., and Romanini, D. (2007). Single–Frequency operation of External–Cavity VCSELs: Non-linear multimode temporal dynamics and quantum limit. *Opt. Express* 15, 9403–9417. doi:10.1364/oe.15.009403

Gil, L., and Lippi, G. L. (2014). Phase instabilities in semiconductor lasers: A codimension-2 analysis. *Phys. Rev. A* 90, 053838. doi:10.1103/physreva.90.053838

Gosset, C., Merghem, K., Martinez, A., Moreau, G., Patriarche, G., Aubin, G., et al. (2006). Subpicosecond pulse generation at 134ghz using a quantum-dash-based fabry-perot laser emitting at 1.56μm. *Appl. Phys. Lett.* 88, 241105. doi:10.1063/1.2213007

Gurevich, S. V., and Javaloyes, J. (2017). Spatial instabilities of light bullets in passively-mode-locked lasers. *Phys. Rev. A* 96, 023821. doi:10.1103/PhysRevA.96.023821

Haus, H. A., and Mecozzi, A. (1993). Noise of mode-locked lasers. *IEEE J. Quantum Electron.* 29, 983–996. doi:10.1109/3.206583

Hausen, J., Lüdge, K., Gurevich, S. V., and Javaloyes, J. (2020). How carrier memory enters the haus master equation of mode-locking. *Opt. Lett.* 45, 6210–6213. doi:10.1364/OL.406136

Hou, L., Haji, M., Akbar, J., Qiu, B., and Bryce, A. C. (2011). Low divergence angle and low jitter 40 ghz algainas/inp 1.55μm mode-locked lasers. *Opt. Lett.* 36, 966–968. doi:10.1364/OL.36.000966

Javaloyes, J., Camelin, P., Marconi, M., and Giudici, M. (2016). Dynamics of localized structures in systems with broken parity symmetry. *Phys. Rev. Lett.* 116, 133901. doi:10.1103/PhysRevLett.116.133901

Jiang, L. A., Ippen, E. P., and Yokoyama, H. (2007). *Semiconductor mode-locked lasers as pulse sources for high bit rate data transmission*. Berlin, Heidelberg: Springer Berlin Heidelberg, 21–51. doi:10.1007/978-3-540-68005-5_2

Keeler, G., Agarwal, D., Nelson, B., Helman, N., and Miller, D. (2003). Performance enhancement of an optical interconnect using short pulses from a modelocked diode laser. Summaries of Papers Presented at the Lasers and Electro-Optics. *CLEO '02. Tech. Diges* (2002), 163 vol.1–. doi:10.1109/CLEO.2002.1033565

Keeler, G., Nelson, B., Agarwal, D., Debaes, C., Helman, N., Bhatnagar, A., et al. (2003). The benefits of ultrashort optical pulses in optically interconnected systems. *IEEE J. Sel. Top. Quantum Electron.* 9, 477–485. doi:10.1109/JSTQE.2003.813317

Maas, D., Bellancourt, A., Rudin, Bea, Golling, M., Unold, H., Sudmeyer, T., et al. (2007). Vertical integration of ultrafast semiconductor lasers. *Appl. Phys. B* 88, 493–497. doi:10.1007/s00340-007-2760-1

Marsh, E. A. Avrutin E. P. J. H., and Portnoi, E. (2000). Monolithic and multi-gigahertz mode-locked semiconductor lasers: Constructions, experiments, models and applications. *IEE Proc. - Optoelectron.* 147, 251–278. doi:10.1049/ip-opt:20000282

Mollenauer, L. F., Mamyshev, P. V., Gripp, J., Neubelt, M. J., Mamysheva, N., Grüner-Nielsen, L., et al. (2000). Demonstration of massive wavelength-division multiplexing over transoceanic distances by use of dispersion-managed solitons. *Opt. Lett.* 25, 704–706. doi:10.1364/OL.25.000704

Paschotta, R., Schlatter, A., Zeller, S., Telle, H., and Keller, U. (2006). Optical phase noise and carrier-envelope offset noise of mode-locked lasers. *Appl. Phys. B Lasers Opt.* 82, 265–273. doi:10.1007/s00340-005-2041-9

Piccardo, M., Schwarz, B., Kazakov, Dea, Beiser, M., Opacak, N., Wang, Y., et al. (2020). Frequency combs induced by phase turbulence. *Nature* 582, 360–364. doi:10.1038/s41586-020-2386-6

Quarterman, A. H., Wilcox, K. G., Elsmere, S. P., Mihoubi, Z., and Tropper, A. C. (2008). Active stabilisation and timing jitter characterisation of sub-500 fs pulse passively modelocked vecsel. *Electron. Lett.* 44, 1135–1137. doi:10.1049/el:20081452

Rosales, R., Murdoch, S. G., Watts, R., Merghem, K., Martinez, A., Lelarge, F., et al. (2012). High performance mode locking characteristics of single section quantum dash lasers. *Opt. Express* 20, 8649–8657. doi:10.1364/OE.20.008649

Sato, K. (2003). Optical pulse generation using fabry-perot lasers under continuous-wave operation. *IEEE J. Sel. Top. Quantum Electron.* 9, 1288–1293. doi:10.1109/JSTQE.2003.819503

Schelte, C., Hessel, D., Javaloyes, J., and Gurevich, S. V. (2020). Dispersive instabilities in passively mode-locked integrated external-cavity surface-emitting lasers. *Phys. Rev. Appl.* 13, 054050. doi:10.1103/PhysRevApplied.13.054050

Scott, R. P., Langrock, C., and Kolner, B. H. (2001). High-dynamic-range laser amplitude and phase noise measurement techniques. *IEEE J. Sel. Top. Quantum Electron.* 7, 641–655. doi:10.1109/2944.974236

Vinogradov, S., Kachanov, A., Kovalenko, S., and Sviridenkov, E. (1992). Nonlinear dynamics of a multimode dye laser with an adjustable resonator dispersion and implications for the sensitivity of intracavity laser spectroscopy. *Jetp Lett. - JETP LETT-ENGL Tr.* 55.

Vladimirov, A., and Turaev, D. (2004). A new model for a mode-locked semiconductor laser. *Radiophys. Quantum Electron.* 47, 769–776. doi:10.1007/s11141-005-0015-8

Wittwer, V. J., Zaugg, C. A., Pallmann, W. P., Oehler, A. E. H., Rudin, B., Hoffmann, M., et al. (2011). Timing jitter characterization of a free-running sesam mode-locked vecsel. *IEEE Photonics J.* 3, 658–664. doi:10.1109/jphot.2011.2160050

Zolotovskii, I. O., Korobko, D. A., and Okhotnikov, O. G. (2015). Frequency modulation of semiconductor disk laser pulses. *Quantum Electron.* 45, 628–634. doi:10.1070/qe2015v045n07abeh015670